Journal of **N**onlinear **A**nalysis and **O**ptimization
Vol. 15, Issue. 1, No.6 : 2024
ISSN : **1906-9685**

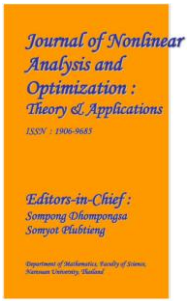

STRUCTURAL PROPERTIES OF CU MG ALLOY NANOPARTICLES: SYNTHESIZED BY WET CHEMICAL PRECIPITATION TECHNIQUE

J. SUBHASHINI, Research scholar, PG & Research Department of Physics, Periyar Arts College, Cuddalore, Tamil Nadu, India
Dr. A. CHRISTY FERDINAND PG & Research Department of Physics, Periyar Arts College, Cuddalore, Tamil Nadu, India Email: christyferdinand2@gmail.com
T. KASTHURY PG & Research Department of Physics, Periyar Arts College, Cuddalore, Tamil Nadu, India.

Abstract

Metaloxide nonmaterial's are important and excellent materials, because of its special properties like chemical stability, high photo catalytic activity, high electric permittivity, non-toxic nature. So it is used in various applications like optical, electrical, electronic, antiseptic, antibacterial, environmental, semiconductors and catalytic devices.

Present work is focused on to synthesis of copper Magnesium alloy Nanoparticles at different annealed temperatures by simple wet chemical Precipitation method. The synthesized copper magnesium alloy nanoparticles have been characterized by X-ray Diffractometer (XRD), Particle Size Analyser (PSA), Scanning Electron Microscope(SEM), ultraviolet-visible spectroscopy (UV VIS),Fourier-transform infrared spectroscopy (FTIR) and CV for structural, average crystallite size, average particle size, morphology, optical properties, chemical bonding and thermal stability respectively.

Key words:
Copper, Magnesium, Alloy Nanoparticles, Chemical precipitation technique

1. INTRODUCTION

Magnesium is renowned for its favorable low-density attributes, rendering it a viable choice for commercial engineering applications in which weight has substantial design implications. Magnesium (Mg) stands as a readily obtainable metallic element, exhibiting robustness, efficient heat dissipation, and excellent damping properties. The utilization of pure magnesium remains infrequent due to its susceptibility to instability under high temperatures and pronounced vulnerability to corrosion within humid environments. Hence, the incorporation of magnesium alloys into the design process of aircraft, automotive, and biomedical applications assumes paramount importance. Magnesium is a strong deoxidizer particularly for nickel alloys. As a Copper master alloy it is effective and less reactive. If alloyed, in can improve mechanical properties. Cu is a less expensive element than several rare earth elements like Nd, Ce, Gd, and Y. [1] Cu, on the other hand, helps to improve the characteristics of Mg alloys. It is commonly accepted that the inclusion of Cu enhances castability and effectively boosts the alloy's eutectic temperature, enabling the complete dissolution of solute atoms at high temperatures. [2, 3] Additionally, the dissolved atoms of the element Cu appear to enhance nucleation, limit grain expansion, and increase precipitate concentration during aging treatment. Because of the refinement of grains generated by Zn and Cu, the alloy Mg–Zn–Cu has been observed to have good ductility and strength. [4] Zhu *et al.*, [5] looked at how copper additions to alloys affected the micro structural features and mechanical qualities of cast ZK60 magnesium alloy products. The results reveal that the addition of the alloying element copper (0.5–1 wt %) to magnesium produces strong mechanical properties, particularly an exceptional elongation percentage of more than 9%. As

a result, at room temperature the mechanical properties of the materials magnesium alloys are highly enhanced due to the variation of the microstructure, which means that the refinement of grains in the microstructures is strongly influenced by the inclusion of copper with magnesium.Liu *et al.*, [6] studied the impact of adding copper as an alloying element with main element magnesium on the microstructural characteristics and mechanical performance of three alloys developed with mixing proportions of copper such as 0.03, 0.19, and 0.57.

2. EXPERIMENTAL PROCEDURES

2.1. Characterization

FTIR spectroscopy (Perkin Elmer, USA) was used in the400–4000cm−1 range for the analysis of chemical compositions of the prepared nano particles. UV–Vis (PerkinElmer) was used to obtain absorbance spectra of the NPs in the range from 200 to800nm. The XRD pattern of Cu Mg alloy was defined utilizing X-ray diffract meter model (Analytical X' pert) using Cu Kα radiation with wave length at λ =1. 5405A. The characteristic of surface morphology such as the particle shape and particle size of Cu Mg alloy nano particles investigated using Phillips XL30 ESEM scanning electronic microscope (SEM). Particle size analyser (Malvern Instruments Ltd Zetasizer Ver. 7.1).

2.2. FTIR studies

The light transmittance properties of the copper magnesium alloy NPs were studied via FTIR as shown in figure1. FTIR, like UV-Vis, enables compounds to be identified given that each compound exhibits distinct transmittance bands when exposed to IR light. The FTIR spectrum of the sample copper magnesium alloy prepared by wet chemical precipitation method is presented in Figure. Figure 1a and 1b shows the FTIR spectra of the sample annealed at two different temperatures namely 300°c and 700°c. It is evident from the figure that, the samples give rise to absorption bands in the range of 4000 to 400 cm^{-1}. The broad band centered at 3422 cm^{-1} can be attributed to the stretching vibrations of O-H functional group. The medium intensity sharp band at 1646 cm^{-1} can be associated with the bending vibrations of O-H functional group. The existence of these two bands confirms the presence of water molecules adsorbed from the environment on the surface of the nanomaterial due to their high specific surface areas [7,8] .The sharp and medium intensity bands at 2923.1 cm^{-1} can be assigned to C-H stretching bonds. These bands invariably appear in the FTIR spectra of samples and they are seldom considered important in determining the structure. The transmittance band at1646 cm-1 is attributed to the C–C stretching mode. Furthermore, the large transmittance band at1385cm-1is ascribed to the C-H bending mode. But not least, the bands in the fingerprinting region between500and700 cm-1could also be attributed to oxygen-metal vibration which hint sat the formation of metal oxides [9].

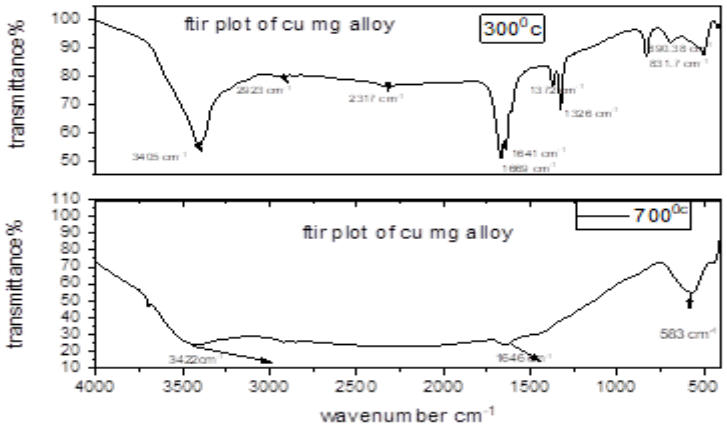

Figure .1 FTIR Plot of Cu Mg alloy at different annealed temperature

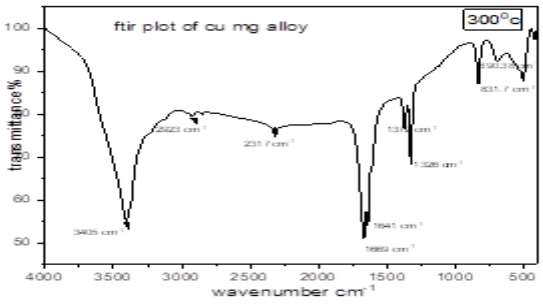

Figure 1a. FTIR Plot of Cu Mg alloy at annealed temperature 300°C

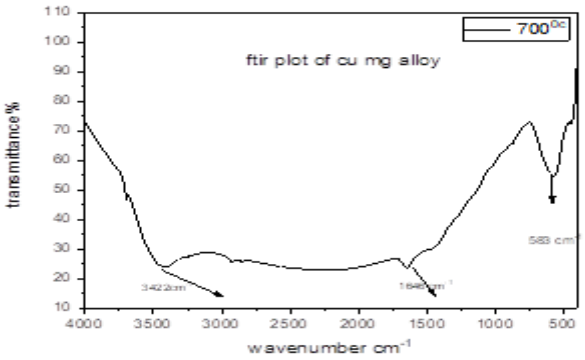

Figure .1b FTIR Plot of Cu Mg alloy at annealed temperature 700°C

2.3. XRD studies

XRD spectra of copper magnesium alloy-NPs obtained from wet chemical precipitation synthesis at different annealed temperatures are shown in (Figure 2).It clearly exhibits the peaksatangles5.6662°, 18.0348°, 23.135°, 26.928°, 28.2086°, 35.4065°, 37.8498°, 43.5339°, 44.4414°, 48.9878°, 51.4988°, 57.2021°, 60.591°and 69.6929° which reveals the information that sharp and intense peaks indicate the synthesized nanoparticles are crystalline in nature. The XRD peak profile analysis is done for as-prepared and annealed copper magnesium alloy sample. Basically, the X-ray line broadening is mainly due to three factors namely instrumental effect, crystalline size and local lattice strain. In order to exclude the instrumental broadening, a standard silicon X-ray powder diffraction data is recorded under the same condition and is eliminated from the observed peak width. But the latter two contributions cannot separate directly and hence Williamson-Hall (W-H) plots are used. The full width at half maximum (FWHM) of all the sample is estimated using a nonlinear curve fitting function called Gaussian, which gives the best fit for the experimental data. As the width of the peak increases size of particle size decreases, which resembles that present material linnanorange [10, 11].

The average crystallite size (D) of the sample is calculated using Debye-Scherer's formula which can be given

$$D = \frac{K\lambda}{\beta COS\theta}$$

where K is the shape factor (0.90), λ is the wavelength of Cu Kαradiation(λ=1.5406Å),β is the full-width a maximum, andθ is the diffraction angle. The average grain size of copper magnesium alloy-NPs is found tobe~27nm and25 nm at different annealed temperatures at 300°C, 700°C respectively. It is seen that the particle grain size decreases with increase in annealed temperatures.

Additionally the dislocation density (δ), which represents the amount of defects in the sample is defined as the length of dislocation lines per unit volume of the crystal and is calculated using Williamson and small man's formula [12] in lines/m^2

$$\delta = \frac{n}{D^2}$$

where n is approximately equal to 1[13], *D* is the crystallite size. The dislocation density (d) is found to be 1.371×1015 lines /m2 and 1.736×1015 lines/m2 sample copper magnesium alloy-NPs different annealed temperatures at 300°C, and 700°C respectively.

2.4. Williamson–Hall Method of Analysis

The Scherrer equation focuses only on the effect of crystallite size in XRD peak broadening and it cannot be considered for microstructures of the lattice, i.e., about the intrinsic strain, which becomes developed in the nano crystals through the point defects, grain boundaries, triple junctions, and stacking faults [14]. One of the methods considering the effect of strain-induced XRD peak broadening is the Williamson–Hall (W-H) method; also, this method provides calculation of the crystal size along with the intrinsic strain [15,16]. According to the physical line broadening of X-ray diffraction peak, it is a combination of size and strain. The W-H method does not confirm a 1/cos θ dependency as in the Scherrer equation but varies with tanθ in strain considerations. This basic difference pursues a dissociation of broadening reflection and combines small crystallite size and micro strain together. The distinguished θ associations of both effects of size and strain broadening in the analysis of W-Haregivenas Equation

$$\beta_{total} = \beta_L + \beta_\epsilon$$

where

$\beta_L = \frac{K\lambda}{LCOS\,\theta}$ and $\beta_\varepsilon = 4C_\epsilon\, tan\theta$

If both contributions are present then their combined effect should be determined by convolution. The simplification of W-H method is to assume the convolution as a simple sum. Using the former of these then we get

$$\beta_{total} = \frac{K\lambda}{LCOS\,\theta} + 4C_\epsilon\, tan\theta$$

If we multiply this equation by cos θ we get:

$$\beta_t cos\theta = \frac{K\lambda}{L} + 4C_\epsilon\, sin\theta$$

Comparing this with the standard equation for a straight line y =mx + c, we see that by plotting β_t cosθ versus 4sinθwe obtain the straight line with the slope Cϵ and the intercept $\frac{K\lambda}{L}$that determines size of the crystal. Such plot is known's W-H plot and shown in (Figure 2a, and 2b). Crystal sizes by W-H plot for copper magnesium alloy-NPs sample at different annealed temperatures 2.1E-10 m, and8.6E-11 respectively. The slope Cϵ gives the micro strain, this may be due to the lattice shrinkage and the values are 0.1799×10^{-3}, ^{3} and 0.6325×10^{-3}

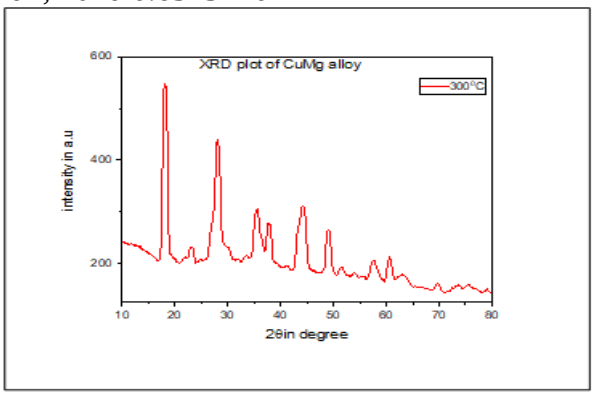

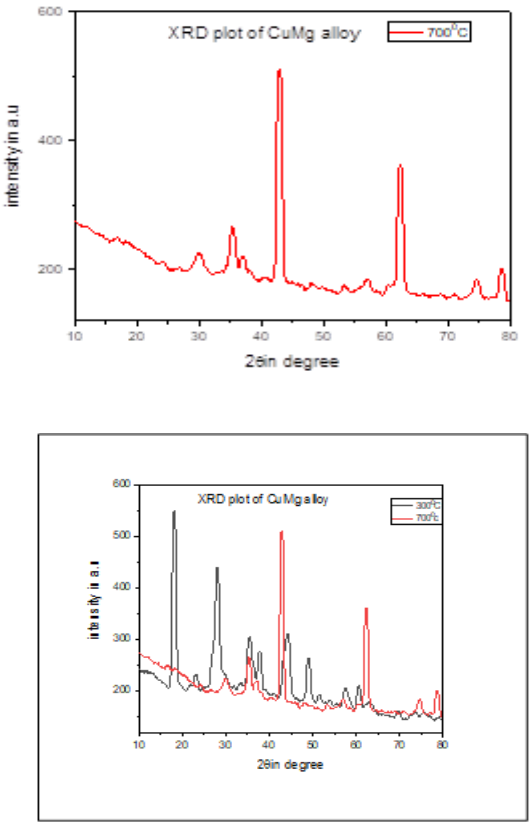

Figure.2 xrd plot of copper magnesium alloy-NPsat different temperatures

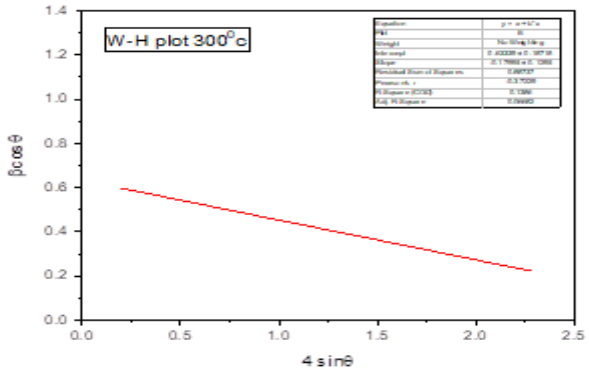

Figure .2a W-H plot for copper magnesium alloy annealed at 300°c

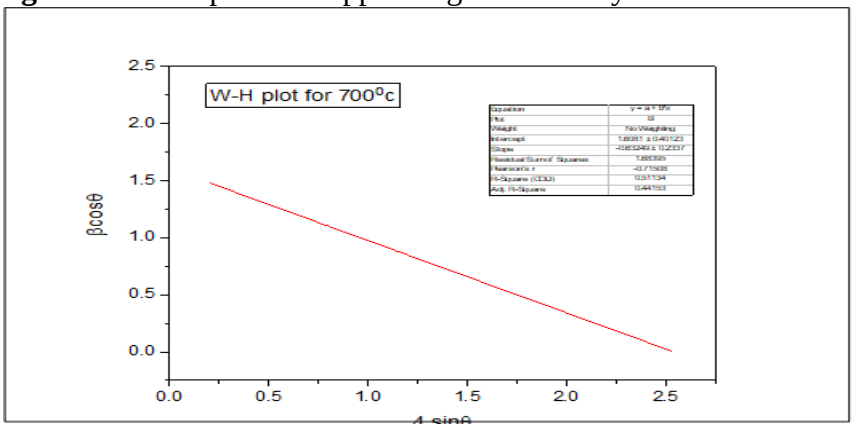

Figure .2b W-H plot for copper magnesium alloy annealed at 700°c

cu mg alloy(300 deg celcuis)					
2θ ιν δεγ	height	fwhm in deg	2θ in rad	fwhm in rad	D=Kλin nm/βCOSθ ιν νμ

5.6662	129.92	1.2595	0.098844	0.021971	6.318408
18.0348	742.43	0.3936	0.314607	0.006866	20.44634
23.135	66.02	0.3149	0.403577	0.005493	25.76352
26.928	122.18	0.2362	0.469744	0.00412	34.60079
28.2086	417.8	0.3149	0.492083	0.005493	26.02452
35.4065	199.62	0.2362	0.617647	0.00412	35.32181
37.8498	205.73	0.2755	0.660269	0.004806	30.49742
43.5339	143.65	0.3149	0.759425	0.005493	27.17652
44.4414	213.05	0.3149	0.775256	0.005493	27.26349
48.9878	195.28	0.1181	0.854565	0.00206	73.95006
51.4988	33.61	0.4723	0.898368	0.008239	18.6822
57.2021	37.78	0.7872	0.997859	0.013732	11.49869
60.591	81.44	0.3936	1.056976	0.006866	23.3842
69.6929	23.73	0.4723	1.215754	0.008239	20.50156
				SUM	381.4295
				AVERAGE	27.24496

4sinθ	**βcosθ**	**slope**	**intercept**	**D=kλ/intercept**
0.197607	1.257962			
0.626622	0.38874	-0.1799	0.6334	2.18904E-10
0.801688	0.308511	micro strain		
0.930874	0.229715			
0.974267	0.305417			
1.215751	0.225026			
1.296681	0.260623			
1.482613	0.29247			
1.511973	0.291537			
1.657597	0.107482			
1.736922	0.425449			
1.913943	0.691237			
2.016913	0.339901			
2.284504	0.387693			

cu mg alloy(700 deg celcuis)					
2θ ιν δεγ	**height**	**fwhm in deg**	**2θ in rad**	**fwhm in rad**	**D=Kλin nm/βCOSθ ιν νμ**
5.8348	186.33	2.2042	0.101785	0.038451	3.610663
29.8992	36.87	0.9446	0.521575	0.016478	8.708955
35.3958	129.68	0.4723	0.61746	0.008239	17.66412
36.912	101.14	0.1574	0.643909	0.002746	53.23274
42.9129	1078.46	0.2362	0.748592	0.00412	36.1539
57.0314	21.58	0.9446	0.994881	0.016478	9.574893
62.2672	539.38	0.1968	1.086217	0.003433	47.17614
74.6947	69.32	0.3149	1.303008	0.005493	31.7425
78.5461	96.38	0.4723	1.370193	0.008239	21.73279
				sum	229.5967
				average	25.51074

4sinθ	βcosθ	slope	intercept	D=kλ/intercept
0.203482	2.201346			
1.031366	0.91266	-0.6325	1.6081	8.62222E-11
1.215396	0.44997	micro strain		
1.265686	0.149313			
1.462469	0.219847			
1.908711	0.830121			
2.067198	0.168482			
2.425531	0.2504			
2.530991	0.365729			

2.5. UV studies

Figure1showstheUV-VISspectrumof synthesised Cu Mg Alloy nanoparticles by wet chemical precipitation method at different temperatures, it reflects the variation of% absorbance of Cu Mg Alloy as a function of wavelength from 200 to 800 nm. The absorbance spectrum fig.1 for cu-Mg alloy conform the presence of alloy or core shells structure cu peak centred at 371 nm and magnesium peak centred at 256 nm Two peaks absorption was observed at 215 nm (1st peak) and 256 nm (2nd peak) . The broad peak was predicted as the Surface Plasmon Resonance (SPR), demonstrating the presence of Cu NPs. In previous studies, Cu NPs showed SPR in an area around 562–573 nm [17, 18, 19]. However, in our work, SPR was observed in the area around 371 nm. It was probably due to the position of Plasmon absorption peak which depends on several factors: the particle size, shape, type of solvent, etc. Literature [20, 21] reveals the broad absorption peaks for MgO nanoparticles prepared by co-precipitation and hydrothermal method are 295nm and297nm at room temperature respectively. On comparisons of the present study with literature reveals that Cu Mg Alloy nanoparticles has led to a shift in the fundamental optical absorption edge towards the Ultra Violet (UV) region. From the spectra, Broad peak around 256 nm shows that the particle possesses quantum confinement [22].This shows that charge particles are confined about three spatial dimensions. The absorption data obtained were extrapolated to the T au c relation: the plot of $(\alpha hv)^2$ versus the energy of the photons (hv), where α is the absorbance value, h is the Plank constant, and ν is the frequency of the photons. When the absorption data are traced by the Tauc relation, it will show one or more straight lines; these lines will intercept with the energy (hv) axis, and this intercept gives the value of the energy gap (Eg) and it is shown in shown in (figure -3).The band gap energy of Cu Mg Alloy nano particle was found to be 5.49 ev, 5.495ev for 300°c and 700°c. The variation of extinction coefficient with wavelength is shown in Figure 3. The extinction coefficient (K) is a measure of the fraction of light lost due to scattering and absorption per unit distance of the penetration medium. The extinction coefficient is computed in the sample during the exposure of UV spectra by using the relation between % absorption and wavelength [23].Extinction coefficient (K) is calculated from the formula

$$K = \frac{\alpha\lambda}{4\pi}$$

where $\alpha$is % absorption and $\lambda$is wavelength. The curve o extinction coefficient clearly shows that scattering decreases gradually from 400 nm up to 1100 nm for constant distance of the penetration medium.

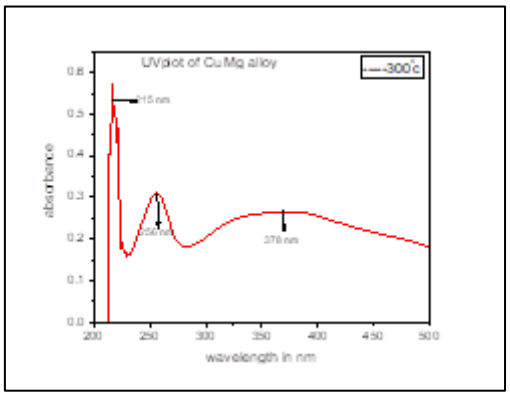
UVplot of Cu Mg alloy
300°c
absorbance
wavelength in nm

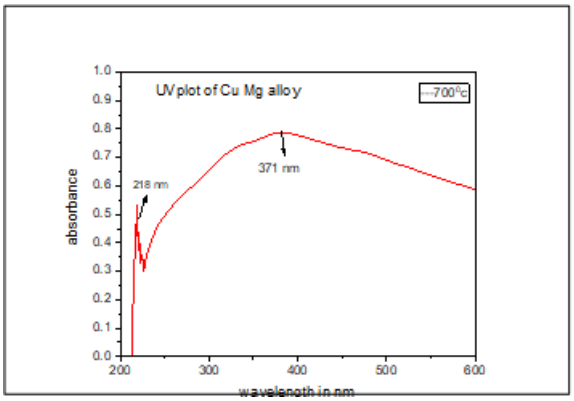
UV plot of Cu Mg alloy
700°c
218 nm
371 nm
absorbance
wavelength in nm

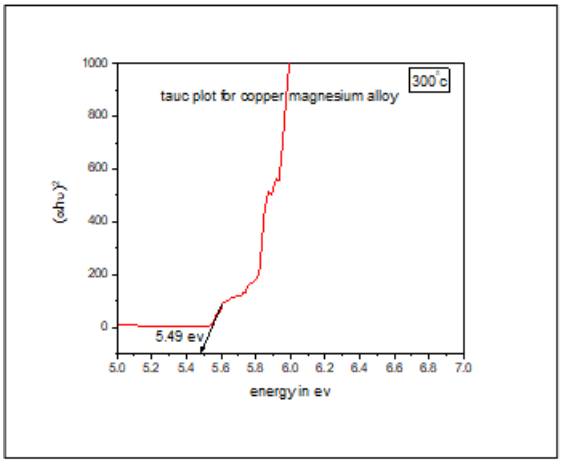
tauc plot for copper magnesium alloy
300°c
5.49 ev
(αhυ)²
energy in ev

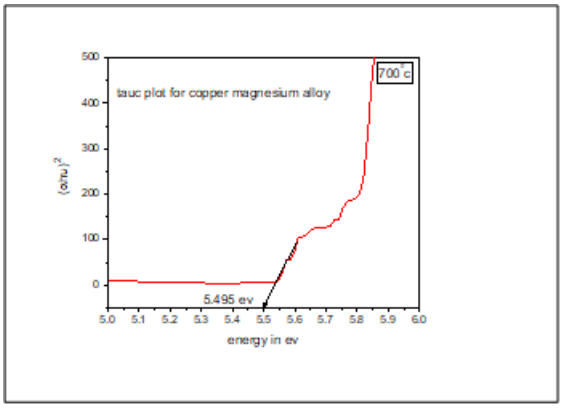
tauc plot for copper magnesium alloy
700°c
5.495 ev
(αhυ)²
energy in ev

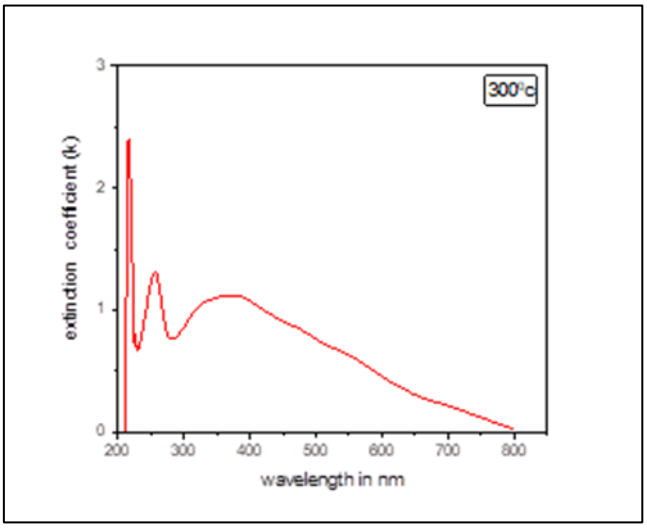

2.6. PSA studies

Copper magnesium alloy nanoparticles samples annealed at two different temperatures 300°c and 700°c were analyzed using particle analyzer to estimate the particle size. Cu Mg alloy nano particles were suspended in water and kept in ultra-sonication for 5min. (Figure 3a and3b) shows the result of the analyzed sample. The average size of the particle was calculated to be 1193 d nm with standard deviation 83.4 for the synthesized Cu Mg alloy nano particles annealed at 300° c and 773.3 d nm with standard deviation106.8 for 700°c at 100%intensity.

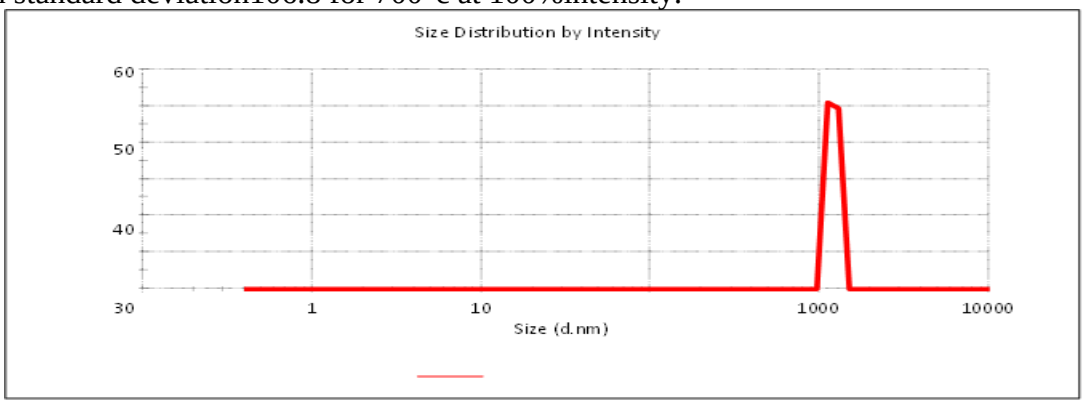

Figure.1a PSA Results of Cu Mg alloy nanoparticles annealed at 300° c

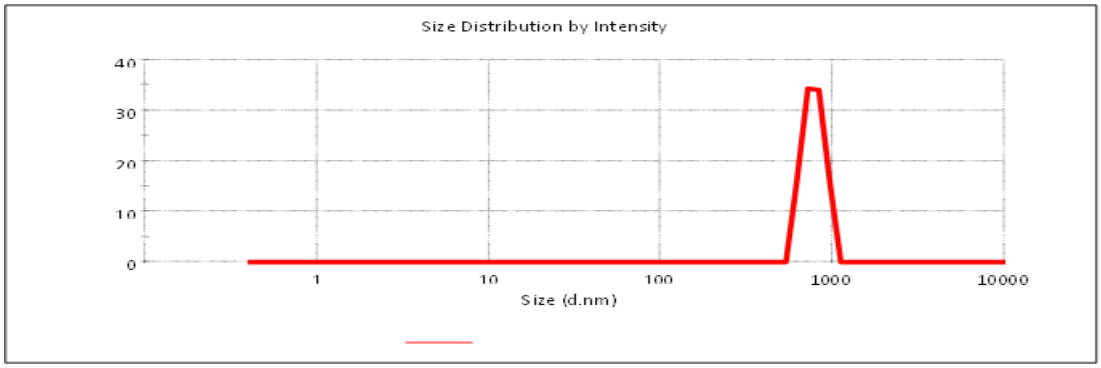

Figure.2a PSA Results ofCu Mg alloy nanoparticles annealed at 700° c

2.7. CYCLIC VOLTAMMETRY RESULTS

The super capacitor properties of the synthesized Cu Mg alloy nanoparticles were determined using cyclic voltammetry. The like voltammetry, were performed at room temperature. Figure 4 (a), 1(b) shows measured cyclic voltammo grams (CVs) recorded in the KOH electrolyte for the synthesized Cu Mg alloy nanoparticles films at four different scan rates (25, 50,75, and 100mVs^{-1}).CVs provide valuable information on reduction oxidation (charge-discharge) behavior. Here, the capacitance was

mainly based on the redox reaction because the shape of the CVs is distinguished from the shape of electric double-layer capacitance, which is normally close to an ideal rectangle [24]. As the scan rate was increased, the current response, which is a measure of the capacitance, increased. The similar shape of the CVs recorded at different scan rates indicates excellent electro chemical reversibility of the synthesized Cu Mg alloy nanoparticles. The specific capacitance of the electrode can be calculated from the CV curves according to the following quation.

$$C=\frac{1}{ms(v_a-v_b)}\int Idv$$

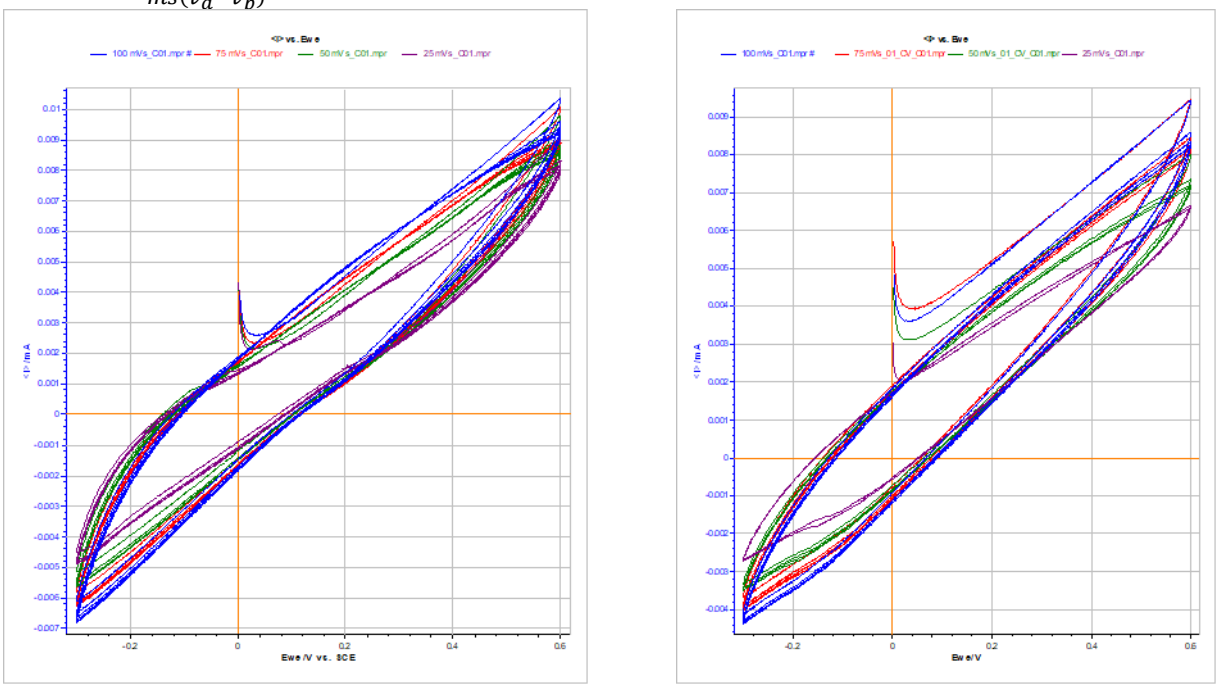

Figure.1 CV Curve of Cu Mg alloy Nanoparticles at Different Scan Rate

2.8. SEM studies

The SEM images of the Cu Mg alloy samples (Fig. 5a and 5b) show that the morphology of particles were almost spherical, regular in shape and dispersed uniformly, but agglomerated symmetrically and the morphology of the single nanoparticles is flake like, the flakes are 54 nm to 57 nm in dimensions for 300°cand 700°c this is to some extent due to the interaction between the nanoparticles, Heat treatment resulted in agglomeration of the powder as a function of the calcining temperature which is typical for the alloy samples. Therefore, some degree of agglomeration at the higher calcinations temperature appears unavoidable. In many cases of Nano crystalline materials, it is observed that there is a tendency of agglomeration among the nanoparticles [28]. Low resolution image of prepared copper magnesium alloy at different temperatures exhibits clusters morphology. High resolution SEM images shows synthesised NPS are grown highly crystalline.

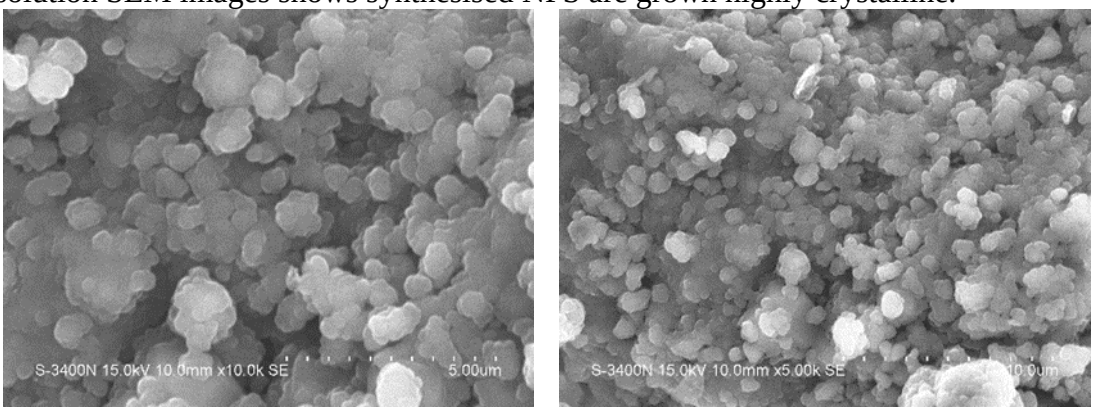

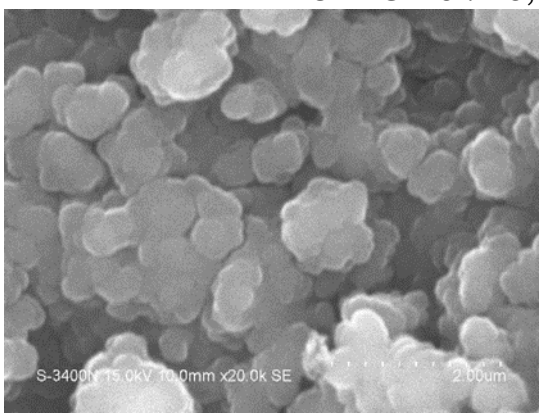

Figure. (5a) Depicts the SEM micrographs of sample Cu Mg alloy nanoparticles for different magnification at 300 ^{0} C

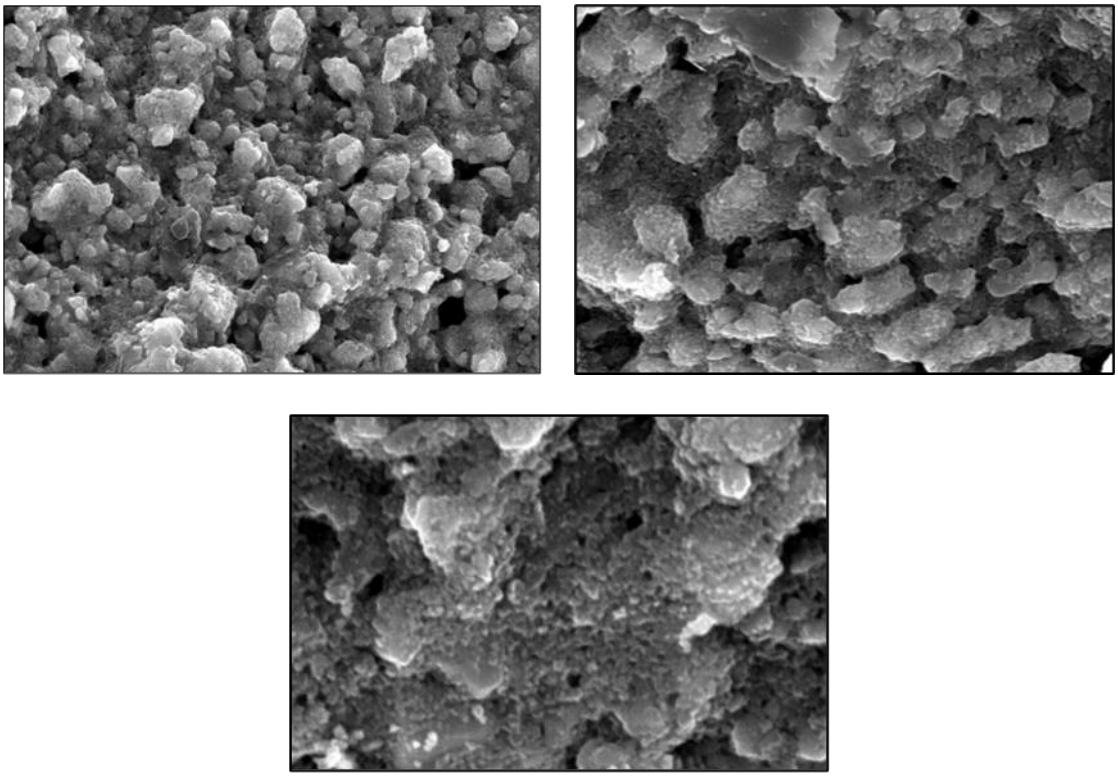

Figure. (5b) Depicts the SEM micrographs of sample Cu Mg alloynanoparticles for different magnification at 700 ^{0} C

REFERENCES

1. Ahmad Reza Abbasian and Mahdi Shafiee Afarani, Onestep solution combustion synthesis and characterization of ZnFe2O4 and ZnFe1.6O4 nanoparticles,J.Appl.Phys.A.125,(2019),1-12.

2. Bakr, N. A. A. M. Funde, V. S. Waman 2011. "Determination of the optical parameters of a-Si:H thin films deposited by hotwire–chemical vapour deposition technique using transmission spectrum only," Pramana: Journal of Physics, vol. 76, no. 3, pp.519–531

3. Buha, J. Mechanical properties of naturally aged Mg-Zn-Cu-Mn alloy. Mater. Sci. Eng. A 2008, 489 (1–2), 127– 137, DOI: 10.1016/j.msea.2007.12.006

4. Dang T.M.D., Le T.T.T., Fribourg-Blanc E., Dang M.C. 2011. Synthesis and optical properties of copper nanoparticles prepared by a chemical reduction method. Adv. Nat. Sci. Nanosci. Nanotechnol.;2(1)

5. Ghosh A, Kumari N, Tewari S, Bhattacharjee A .2013. Structural andoptical properties of pure And Aldoped ZnO nanocrystals. Indian JPhys87:1099–1104.https://doi.org/10.1007/s1264 013-0346-9

6. Golmakaniyoon, S.; Mahmudi, R. Microstructure and creep behaviour of the rare-earth-doped Mg-6Zn-3Cu cast alloy. Mater. Sci. Eng. A 2011, 528 (3), 1668– 1677, DOI: 10.1016/j.msea.2010.10.095
7. Hemmati, S.Ahany Kamangar,A. Ahmeda,M.M.Zangeneh,A.Zangeneh, Application of copper nanoparticles containing natural compounds in the treatment of bacterial and fungal diseases,Appl.OrganometChem.34(2020)1–16,https://doi.org/10.1002/aoc.5465.
8. Inamdar, A. I. Y. S. Kim, S. M. Pawar, J. H. Kim, H.Im and H. Kim, J. PowerSources(2011),196, 239.
9. Jacob,R.;Isac,J. 2015.X-ray diffraction line profile analysis of Ba0. 6Sr0. 4 Fex Ti (1−x)O3-δ, (x=0.4).Int.J.Chem.Stud.,2, 12–21.
10. Kandiban, M. P.VigneshwaranandI.Vetha Potheher,2015. Synthesis and Characterization of Mgo Nanoparticles for the catalytic Applications: jan
11. Liu, C.; Fu, X.; Pan, H.; Wan, P.; Wang, L.; Tan, L.; Wang, K.; Zhao, Y.; Yang, K.; Chu, P. K. Biodegradable Mg-Cu alloys with enhanced osteogenesis, angiogenesis, and long-lasting antibacterial effects. Sci. Rep. 2016, 6, 27374, DOI: 10.1038/srep27374
12. Nath, D.Singh,F. Das, 2019. R.X-ray diffraction analysis by Williamson-Hall, Halder- Wagner and size-strainp lot methods of CdSe nanoparticle-A comparative study. Mater.Chem.Phys., 239,122021.
13. Nemade K. R. and S. A. Waghuley, 2013. "UV–VIS spectroscopicstudy of one pot synthesized strontium oxide quantum dots, "Results in Physics,vol.3, pp.52–54
14. Palusamy Suppuraj, Ganesamoorthy Thirunarayanan, Meenakshi sundaram Swaminathan and Inbasekaran Muthuvel, FacileSynthesis ofSpinel Nanocrystalline ZnFe2O4:Enhanced Photocatalytic and Microbial Applications,J.MaterSciTechnol,34,(2017)5-11.
15. Patil, H. S.; Patel, D. C., 2021.Age hardening heat treatment behavior of the as cast Mg–Zn–Al alloys. Frat. IntegritaStrutt., 15 (57), 350– 358, DOI: 10.3221/IGF-ESIS.57.25
16. Rameshwar Rao, V.Rajendar and K. Venkateswara Rao,"Structural and Optical Properties of ZnO NanoParticles Synthesised by Mixture of Fuel Approach in Solution Chemical Combustion," Advanced MaterialsResearch,629, pp.273-278,2013.
17.Rastogi C K,Sala,S, Sivakumar S,Pala R G S and Kumar J 2015 Ph.Chem,Chem Phys 17,4600-4608.
18. Sampath M., Vijayan R., Tamilarasu E., Tamilselvan A., Sengottuvelan B. 2014. Green synthesis of novel jasmine bud-shaped copper nanoparticles. J. Nanotechnol. 2014:1–7.
19. Srivastava, M. S. Chaubey, K. O. 2009.Animesh, Mater. Chem. Phy. 118, 174.
20. Suci Amaliyah,a Dwika Putri Pangesti,a Masruri Masruri,a Akhmad Sabarudin,a,∗ and Sutiman Bambang Sumitrob, 2020. Green synthesis and characterization of copper nanoparticles using Piper retrofractum Vahl extract as bioreductor and capping agentPublished online Aug 7. doi: 10.1016/j.heliyon.2020.e04636
21. Tamizh Selvi,M. Rathnakumari, M.Priyaand P. Suresh Kumar, 2014 .Shape Transition Effect of Temperature on MgO Nanostructures and its Optical Properties," International Journal of Scientific &Engineering Research, 5,pp. 60-64.
22. Velumani S, Narayandass Sa K, Mangalaraj D (1998). Structural characterization of hot wall Deposited selenide thin films. Semicond Sci Technol13(1016–10):24
23. Yu, H.; Yu, H.-sS.; Kim, Y.-M.; You, B.-S.; Min, G.-H., 2013.Hot deformation behaviour and processing maps of Mg-Zn-Cu-Zr magnesium alloy. Trans. Nonferrous Met. Soc. China, 23 (3), 756–764, DOI: 10.1016/S1003-6326(13)62526-1
24. Zhu, H.-m.; Luo, C.-p.; Liu, J.-w.; Jiao, D.-l. 2014. Effects of Cu addition on microstructure and mechanical properties of as-cast magnesium alloy ZK60. Trans. Nonferrous Met. Soc. China, 24 (3), 605– 610, DOI: 10.1016/S1003-6326(14) 63101-0